



# Fabrication of an AMC/MMT Fluorescence Composite for its Detection of Cr(VI) in Water

Yanke Wei<sup>1</sup>, Lefu Mei<sup>1\*</sup>, Rui Li<sup>2</sup>, Meng Liu<sup>1</sup>, Guocheng Lv<sup>1\*</sup>, Jianle Weng<sup>1</sup>, Libing Liao<sup>1\*</sup>, Zhaohui Li<sup>1,3</sup> and Lin Lu<sup>2</sup>

<sup>1</sup> Beijing Key Laboratory of Materials Utilization of Nonmetallic Minerals and Solid Wastes, National Laboratory of Mineral Materials, School of Materials Science and Technology, China University of Geosciences, Beijing, China, <sup>2</sup> State Grid Corporation of China, Beijing, China, <sup>3</sup> Geosciences Department, University of Wisconsin—Parkside, Kenosha, WI, United States

## OPEN ACCESS

### Edited by:

Wenbo Wang,  
Lanzhou Institute of Chemical Physics  
(CAS), China

### Reviewed by:

Liang Bian,  
Southwest University of Science and  
Technology, China  
Runliang Zhu,  
Guangzhou Institute of Geochemistry  
(CAS), China

### \*Correspondence:

Lefu Mei  
mlf@cugb.edu.cn  
Guocheng Lv  
guochenglv@cugb.edu.cn  
Libing Liao  
clayl@cugb.edu.cn

### Specialty section:

This article was submitted to  
Green and Sustainable Chemistry,  
a section of the journal  
Frontiers in Chemistry

Received: 07 June 2018

Accepted: 30 July 2018

Published: 21 August 2018

### Citation:

Wei Y, Mei L, Li R, Liu M, Lv G,  
Weng J, Liao L, Li Z and Lu L (2018)  
Fabrication of an AMC/MMT  
Fluorescence Composite for its  
Detection of Cr(VI) in Water.  
Front. Chem. 6:367.  
doi: 10.3389/fchem.2018.00367

Hexavalent chromium species, Cr(VI), which can activate teratogenic processes, disturb DNA synthesis and induce mutagenic changes resulting in malignant tumors. The detection and quantification of Cr(VI) is very necessary. One of the rapid and simple methods for contaminant analysis is fluorescence detection using organic dye molecules. Its application is limited owing to concentration quenching due to aggregation of fluorescent molecules. In this study, we successfully intercalated 7-amino-4-methylcoumarin (AMC) into the interlayer space of montmorillonite (MMT), significantly inhibited fluorescence quenching. Due to enhanced fluorescence property, the composite was fabricated into a film with chitosan to detect Cr(VI) in water. Cr(VI) can be detected in aqueous solution by instruments excellent, ranging from 0.005 to 100 mM with a detection limit of 5  $\mu$ M.

**Keywords:** AMC/MMT composite, fluorescence, quenching, detection, hexavalent chromium

## INTRODUCTION

Due to the high toxicity of heavy metals and bioaccumulation in human body through the food chain, will bring human health and environmental great issue. Cr is one of the most serious contaminants among various heavy metals (Soewu et al., 2014; Wu et al., 2015a; Širić et al., 2017). While Cr(III) is an essential micronutrient, Cr(VI) is toxic (Weibel et al., 2016). Cr(VI) is mainly produced by electroplating, leather tanning, and textile dyeing (Dehghani et al., 2016; Omorogie et al., 2016). Cr(VI) is the most virulent form (Miretzky and Cirelli, 2010) of Cr, which is a highly toxic agent and act as carcinogens, mutagens, and teratogens in biological systems (Hlihor et al., 2017; Mullick et al., 2017). The carcinogenic and toxicity of Cr(VI) is based on its oxidation states like the most transition metals (Yusof and Malek, 2009; Kumar et al., 2017). An effective, simple and low-cost method for detecting Cr(VI) is needed (Babu and Gupta, 2008; Wang G. et al., 2017). The classic methods for detecting Cr(VI) include electrochemical method, atomic absorption method and liquid chromatography (Anthemidis et al., 2002; De Ruiter et al., 2008). These methods are credible. However, the processes are complicated. Due to its sensitivity, fluorescence spectroscopy has become one of the most increasingly used techniques (Wang et al., 2015; Li and Wei, 2017). The sensors made of organic or inorganic materials show great promise in detection, lighting, and other application (Rao et al., 2014).

Montmorillonite is a typical phyllosilicate of the smectite group of clay minerals (Ismadji et al., 2016; Xu et al., 2016). It consists of two layers of silicon tetrahedron (T) and the middle layer of aluminum octahedron (O) (Bekri-Abbes and Srasra, 2016; Scholtzová et al., 2016; Wang W. et al., 2017). Because of the isomorphous replacement of  $\text{Al}^{3+}$  by  $\text{Mg}^{2+}$  and  $\text{Fe}^{2+}$  in the octahedral sites and  $\text{Si}^{4+}$  by  $\text{Al}^{3+}$  in the tetrahedral sites, TOT layers are negative electric charge, balanced by the cations such as  $\text{Ca}^{2+}$  and  $\text{Na}^{+}$  intercalate into the layers (Dominijanni and Manassero, 2012; Wu et al., 2016; Zhou et al., 2016). Luminescent materials of small organic molecules are easily modified and chemically purified to have wider emission spectrum coverage (Wu et al., 2015b; Tian et al., 2017). However, when they are applied in solid devices, stabilize and enhance their luminous intensity is crucial. Although several methods of assembling materials have been developed (Zhang et al., 2005), they often suffer from phase separation, agminated organic small molecules (Wei et al., 2016; De Sa et al., 2017). Clay minerals were rarely used as base materials for the organic-inorganic composite preparation for luminescence and fluorescence applications.

This research focused on the fabrication of a fluorescence material for Cr(VI) detection. To prevent quenching, the photoactive organic dye AMC was interposed into the interlining of MMT for maximal dye separation and minimum agminated (Yu et al., 2013, 2014). The AMC/MMT was fabricated in a film with chitosan. Quenching of fluorescence was used various solutions to be evaluated. The response of AMC/MMT composites in Cr(VI) was excellent, ranging from 0.005 to 100 mM.

## MATERIALS AND METHODS

### Materials

The montmorillonite was bought from Ningcheng, Inner Mongolia, China. Its CEC (Cation Exchange Capacity) was 9.8  $\text{mmol}_c/10\text{ g}$  which used  $\text{Na}^{+}$  as the staple commutable cation

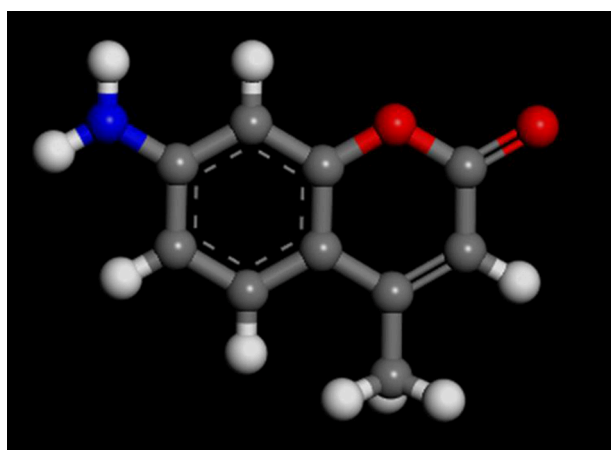


**FIGURE 1** | Molecular structure of AMC studied. The all strains, C, gray; N, blue; O, red; H, white.

exchange. The specific external surface area was  $78\text{ m}^2/\text{g}$ . AMC was purchased from Aladdin. The molecular structure (Nowakowska et al., 2001) of AMC is presented in **Figure 1**. The potassium dichromate Cr(VI), chitosan, and other reagents were purchased from various manufactures that were all of analytical grade. Deionized water was used as a solvent.

### Preparation of AMC/MMT

The effect of initial AMC concentrations on a performance of fluorescence were tested, 50 mL the original concentrations of AMC in water for 20, 50, 100, 200, 500, and 800 mg/L were blended with 0.25 g of MMT in every 100 mL centrifugal tube after shaking at 200 rotations per minute at indoor temperature for 8 h, respectively. The admixtures were centrifuged at 7,500 rotations per minute for 2 min. Afterwards, removing the supernatant, then at  $60^\circ\text{C}$  were dried the residues and pulverized the residues to powder as raw materials. This type of product was used for the AMC/MMT.

### Preparation of the Chitosan Film (AMF) for Cr(VI) Detection in Water

The chitosan film was prepared as follows: 0.25 g chitosan, 8 mL 0.1 M NaOH solution, 0.1 g AMC/MMT powder and two drops of 1 g/mL Polyvinyl Alcohol (PVA) solution were appended. The

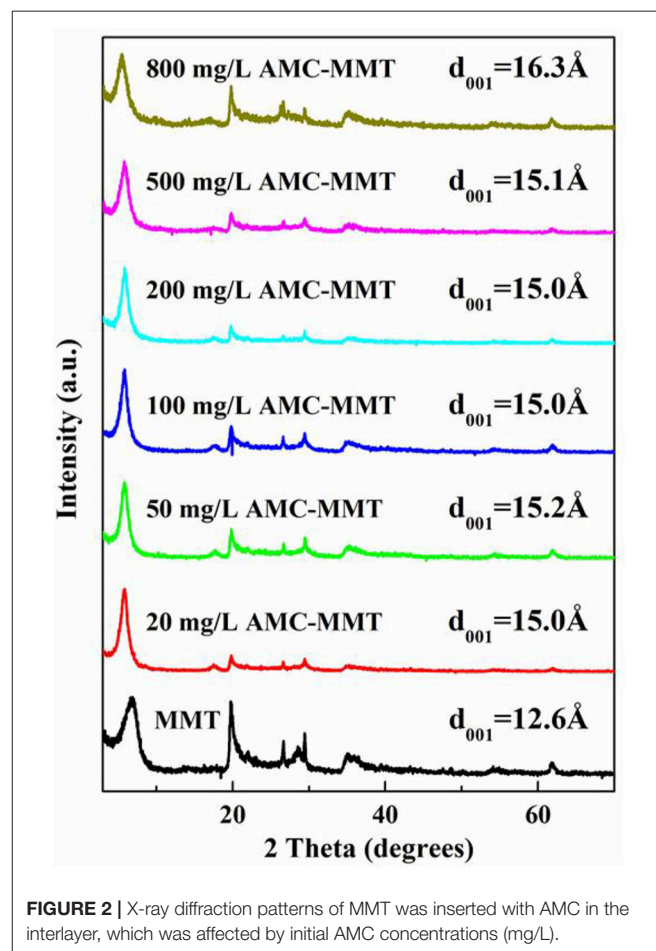


**FIGURE 2** | X-ray diffraction patterns of MMT was inserted with AMC in the interlayer, which was affected by initial AMC concentrations (mg/L).

admixture was whipped for 30 min and then poured into a mold and air dried.

The followed solutions at a concentration of 0.1 M were originally screened for quenching of fluorescence in AMF:  $\text{Al}^{3+}$ ,  $\text{Ca}^{2+}$ ,  $\text{Ba}^{2+}$ ,  $\text{Cr(VI)}$ , CTAB,  $\text{K}^+$ ,  $\text{Na}^+$ ,  $\text{Ni}^{3+}$ ,  $\text{Pb}^{2+}$ ,  $\text{Fe}^{3+}$ , Imidazole,  $\text{C}_2\text{H}_5\text{OH}$ . Afterwards, they were dropped onto the AMF. Then, the fluorescence degrees were measured using a fluorescence spectrophotometer (Hitachi, F4600).

In order to estimate the Cr(VI) range of response, different concentrations of Cr(VI) solution were dropped onto the AMF. The Cr(VI) of original concentrations were the ranged of 5  $\mu\text{M}$  to 100 mM.

Pictures of the AMF after in contact with Cr(VI) solutions were already obvious demonstration quenching of fluorescence effect by Cr(VI) and then measure the florescence intensions of AMF by fluorescence spectrophotometer (Hitachi, F4600).

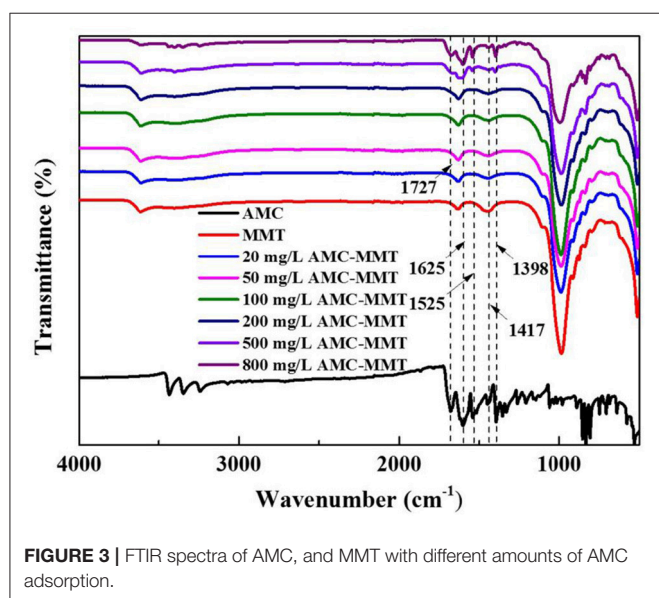


**FIGURE 3** | FTIR spectra of AMC, and MMT with different amounts of AMC adsorption.

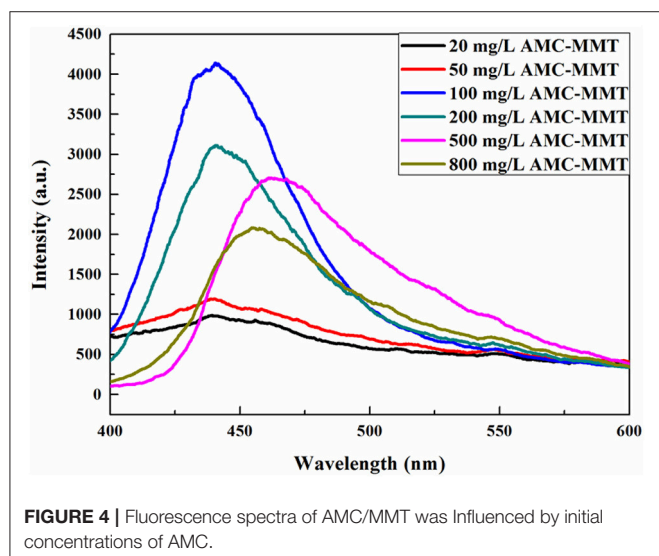


**FIGURE 4** | Fluorescence spectra of AMC/MMT was influenced by initial concentrations of AMC.

## Instrumental Analyses

Powder X-Ray Diffraction (XRD) was performed by a Rigaku D/max-IIIa diffractometer (Tokyo, Japan) with a Ni-filtered Cu K $\alpha$  radiation at 40 kV and 40 mA. Prototypes were scanned the range of 3° to 70° at 8° per minute with a pace of 0.01° to research the particular changes in  $d_{001}$  separation distance of MMT as a function of original AMC concentrations. The changing of peak position proved the intercalation of AMC into the MMT was succeeded. The gallery heights were deduced from the (001) reflection of the composites using the Bragg's equation.

Fourier Transform Infrared Spectroscopy (FTIR) spectra were acquired on a Perkin Elmer Spectrum 100 Spectrometer. The spectra were obtained from 4,000 to 500  $\text{cm}^{-1}$  by adding 256 scans in the resolution ratio of 4  $\text{cm}^{-1}$ .

Photoluminescence emission (PL) spectrum was obtained on a fluorescence spectrophotometer (Hitachi, F4600) at the scope of 400–600 nm with a photomultiplier tube handled at 800 volt. A 150 watt xenon lamp was served as the pumping source, at an excitation wavelength of 340 nm (Zamojć et al., 2015). The emission and excitation slits size were 5 nm and scan speed was setting at 240 nm per min.

Molecular mimicry was performed at the standard module “Forcite” of Materials Studio 6.0 software to research the structure of AMC in the interval of MMT. The unit lattice parameters were setted at  $a = 1.55 \text{ nm}$ ,  $b = 1.79 \text{ nm}$ ,  $c = 1.25 \text{ nm}$ ,  $\alpha = \gamma = 90^\circ$ , and  $\beta = 99^\circ$ . A suite of  $2 \times 2 \times 1$  supercells were constructed of the interlayer spacing setting at 1.63 nm. Every circulation consisted of  $10^6$  steps, repeating three cycles.

## RESULTS AND DISSCUSSION

### The MMT Was Intercalated With AMC

The idea that interlayer cation was  $\text{Na}^+$  with a monolayer hydration was confirmed because the  $d_{001}$  value of pure MMT was 12.6 Å. The  $d_{001}$  spacing progressively increased from 12.6 to 16.3 Å with the initial AMC concentration increased (Figure 2),

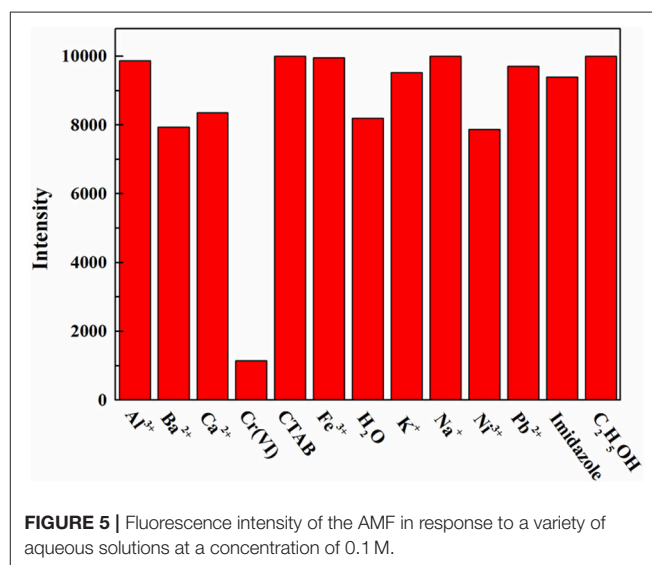
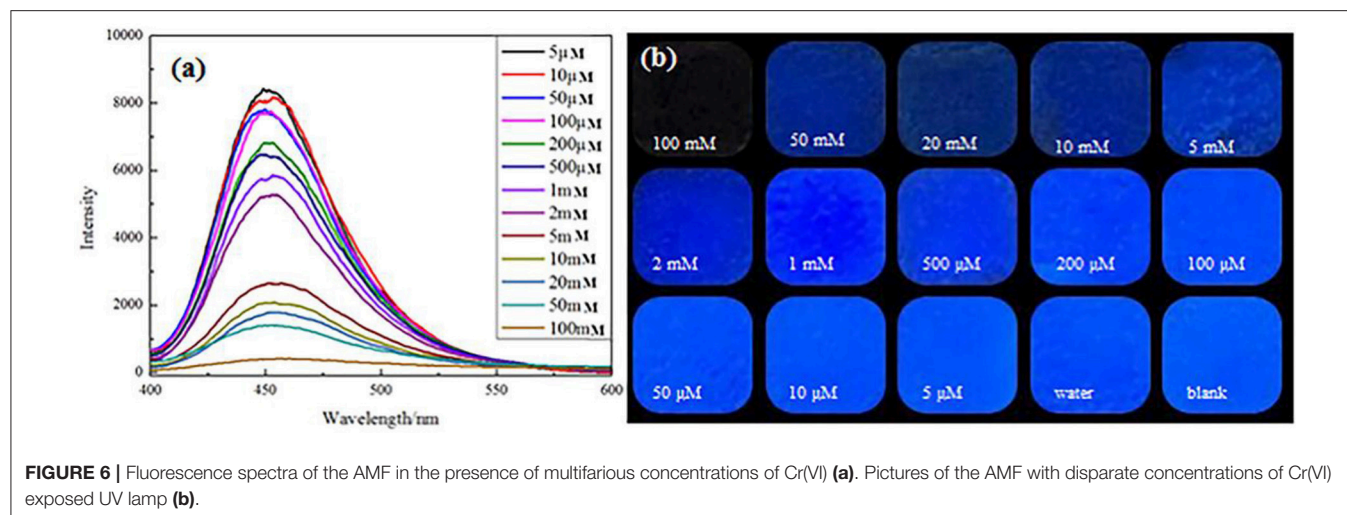


**FIGURE 5** | Fluorescence intensity of the AMF in response to a variety of aqueous solutions at a concentration of 0.1 M.



suggesting AMC molecules insert the portion between the interlayer space of MMT.

### FTIR Spectra of AMC/MMT

FTIR spectra of MMT adsorbed with different amounts of AMC displayed both bands of raw MMT and AMC (Figure 3). The bands between 1,400 and 1,650  $\text{cm}^{-1}$  were allocated to C-C stretching vibrations in aromatic and hetero aromatic compounds (Talbi et al., 1998; Krishnakumar and Xavier, 2005). Therefore, the bands observed at 1,727, 1,695, 1,625, 1,566, 1,525, 1,475, 1,446, 1,417, 1,398, 1,390  $\text{cm}^{-1}$  in FTIR spectra were allocated to C-C stretching vibrations of AMC (Arivazhagana et al., 2010). The characteristic peaks of AMC appeared in FTIR spectra of AMC/MMT, as shown in the dotted line (Figure 3), indicating that AMC had been loaded onto MMT.

### Luminescence Properties of AMC/MMT

AMC powder was hardly used as a luminescent material just because the lack of strong luminescence (Wang et al., 2012), causing by concentration quenching (Wu et al., 2015b). The luminous intensity increased significantly after the intercalation of AMC into the interlayer of MMT, which reason was AMC was uniformly dispersed on MMT, inhibiting its aggregation. The highest spectral intensity was found by AMC/MMT at 100 mg/L, which was an initial concentration (Figure 4).

### The Fluorescent Detection of Cr(VI) in Aqueous Phase by AMF

The AMF was screened for response to various solutes (Figure 5). The fluorescence response to Cr(VI) was very significant when the test solute with an initial concentration of 0.1 M, while others were not obvious, indicating the high selectivity of AMF for Cr(VI).

The mechanism of photoluminescence (PL) quenching of AFM was further investigated when the aqueous solution contains Cr(VI). Most importantly, an apparent decrease

in fluorescence intensity was observed while the Cr(VI) concentration was increasing over the whole concentration ranges from 0.005 to 100 mM (Figure 6a). A full PL quenching process can be observed visually at a Cr(VI) concentration of 1 mM. The images of AMF with addition of Cr(VI) that exposed ultraviolet light showed a consistent tendency (Figure 6b).

### Mechanism Analysis

Molecular mimicry was performed at the standard module “Forcite” of Materials Studio 6.0 software to research the structure of AMC between the interval of MMT. The interlayer spacing of MMT was directly influenced by the interlayer arrangement of AMC and the amount of AMC intercalation, this, on the other hand, would play a significant role in understanding the system structure and interaction forces (Krauss et al., 2011; Wang et al., 2011; Tournassat et al., 2016). The interlayer condition of AMC interpolation MMT with different quantities was qualitatively simulated, and the initial states were represented by a, c, and e; and b, d, and f represent the states after simulation (a stands for low concentration; c stands for medium concentration; and e stands for higher concentration; Figure 7). The concentration quenching could be effectively avoided by AMC intercalation MMT and it could also significantly improve luminous intensity, lifespan, and stability notably owing to the stronger interaction forces between AMC molecules and MMT sheet (Yan et al., 2010a,b; Liu et al., 2014).

### CONCLUSIONS

In this research, an organic dye (AMC) was resoundingly intercalated into the interlayer space of MMT, resulting in observably inhibition in quenching of fluorescence. The composite was fabricated into a film with chitosan to detect Cr(VI) in water with its enhanced fluorescent property. Cr(VI) can be detected in aqueous solution by instruments

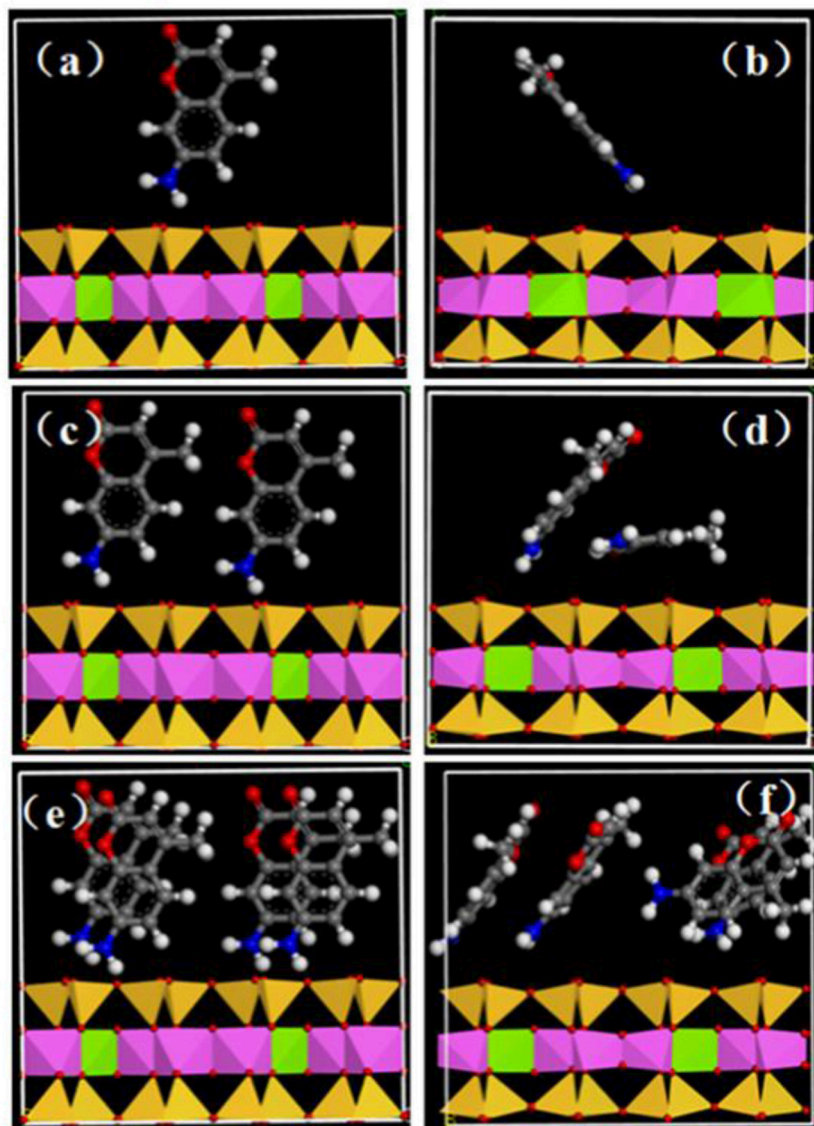


**FIGURE 7** | Dynamic simulation of molecular interposition AMC into MMT at a different angle on account of the electric density and AMC loading distinction. The initial states were represented by **a**, **c**, and **e**; and **b**, **d**, and **f** represent the states after simulation: **a** stands for low concentration, **c** stands for medium concentration and **e** stands for higher concentration. The all strains, Mg, green; Al, pink; Si, yellow; C, gray; N, blue; O, red; H, white.

ranging from 0.005 to 100 mM with a detection limit of 5  $\mu$ M.

## AUTHOR CONTRIBUTIONS

YW and LM conceived the project. LM, GL, and LibL designed and performed the experiments. RL, ML, JW, and LinL analyzed the data. YW, ZL, and LM wrote the manuscript.

## FUNDING

This research was supported by National Natural Science Foundation of China (grant number: 51604248), the National Key R&D Program of China (grant number: 2017YFB0310704), and Fundamental Research Funds for the Central Universities (grant numbers: 2652017335, 2652017338 and 2652017366).

## REFERENCES

- Anthemidis, A. N., Zachariadis, G. A., Kougoulis, J. S., and Stratis, J. A. (2002). Flame atomic absorption spectrometric determination of chromium (VI) by on-line preconcentration system using a PTFE packed column. *Talanta* 57, 15–22. doi: 10.1016/S0039-9140(01)00676-2
- Arivazhagana, M., Sambathkumar, K., and Jeyavijayanc, S. (2010). Density functional theory study of FTIR and FT-Raman spectra of 7-acetoxy-4-methyl coumarin. *Indian J. Pure Appl. Phys.* 48, 716–722. doi: 10.13140/RG.2.1.4538.7361
- Babu, B. V., and Gupta, S. (2008). Adsorption of Cr (VI) using activated neem leaves: kinetic studies. *Adsorption* 14, 85–92. doi: 10.1007/s10450-007-9057-x
- Bekri-Abbes, I., and Srasra, E. (2016). Effect of mechanochemical treatment on structure and electrical properties of montmorillonite. *J. Alloys Compd.* 671, 34–42. doi: 10.1016/j.jallcom.2016.02.048
- De Ruiter, G., Gupta, T., and Van Der Boom, M. E. (2008). Selective optical recognition and quantification of parts per million levels of Cr<sup>6+</sup> in aqueous and organic media by immobilized polypyridyl complexes on glass. *J. Am. Chem. Soc.* 130, 2744–2745. doi: 10.1021/ja7110527
- De Sa, A., Moura, I., Abreu, A. S., Oliveira, M., Ferreira, M. F., and Machado, A. V. (2017). High fluorescent water soluble CdTe quantum dots—a promising system for light harvesting applications. *J. Nanopart. Res.* 19:180. doi: 10.1007/s11051-017-3872-0
- Dehghani, M. H., Sanaei, D., Ali, I., and Bhatnagar, A. (2016). Removal of chromium (VI) from aqueous solution using treated waste newspaper as a low-cost adsorbent: kinetic modeling and isotherm studies. *J. Mol. Liq.* 215, 671–679. doi: 10.1016/j.molliq.2015.12.057
- Dominijanni, A., and Manassero, M. (2012). Modelling the swelling and osmotic properties of clay soils. Part II: the physical approach. *Int. J. Eng. Sci.* 51, 51–73. doi: 10.1016/j.ijengsci.2011.11.001
- Hlihor, R. M., Figueiredo, H., Tavares, T., and Gavrilescu, M. (2017). Biosorption potential of dead and living *Arthrobacter viscosus* biomass in the removal of Cr (VI): batch and column studies. *Process Safe. Environ. Prot.* 108, 44–56. doi: 10.1016/j.psep.2016.06.016
- Ismadji, S., Tong, D. S., Soetedjo, F. E., Ayucitra, A., Yu, W. H., and Zhou, C. H. (2016). Bentonite hydrochar composite for removal of ammonium from Koi fish tank. *Appl. Clay Sci.* 119, 146–154. doi: 10.1016/j.clay.2015.08.022
- Krauss, T. N., Barrena, E., Lohmüller, T., Spatz, J. P., and Dosch, H. (2011). Growth mechanisms of phthalocyanine nanowires induced by Au nanoparticle templates. *Phys. Chem. Chem. Phys.* 13, 5940–5944. doi: 10.1039/C0CP02191A
- Krishnakumar, V., and Xavier, R. J. (2005). Density functional theory calculations and vibrational spectra of 3, 5-dibromopyridine and 3, 5-dichloro-2, 4, 6-trifluoropyridine. *Spectrochim. Acta Part A Mol. Biomol. Spectrosc.* 61, 253–260. doi: 10.1016/j.saa.2004.03.038
- Kumar, R., Kim, S. J., Kim, K. H., Lee, S. H., Park, H. S., and Jeon, B. H. (2017). Removal of hazardous hexavalent chromium from aqueous phase using zirconium oxide-immobilized alginate beads. *Appl. Geochem.* 88, 113–121. doi: 10.1016/j.apgeochem.2017.04.002
- Li, C., and Wei, C. (2017). DNA-templated silver nanocluster as a label-free fluorescent probe for the highly sensitive and selective detection of mercury ions. *Sens. Actuat. B Chem.* 242, 563–568. doi: 10.1016/j.snb.2016.11.091
- Liu, M., Wang, T., Ma, H., Fu, Y., Hu, K., and Guan, C. (2014). Assembly of luminescent ordered multilayer thin-films based on oppositely-charged MMT and magnetic NiFe-LDHs nanosheets with ultra-long lifetimes. *Sci. Rep.* 4:7147. doi: 10.1038/srep07147
- Miretzky, P., and Cirelli, A. F. (2010). Cr (VI) and Cr (III) removal from aqueous solution by raw and modified lignocellulosic materials: a review. *J. Hazard. Mater.* 180, 1–19. doi: 10.1016/j.jhazmat.2010.04.060
- Mullick, A., Moulik, S., and Bhattacharjee, S. (2017). Removal of hexavalent chromium from aqueous solutions by low-cost rice husk-based activated carbon: kinetic and thermodynamic studies. *Indian Chem. Eng.* 60, 58–71. doi: 10.1080/00194506.2017.1288173
- Nowakowska, M., Smoluch, M., and Sendor, D. (2001). The effect of cyclodextrins on the photochemical stability of 7-amino-4-methylcoumarin in aqueous solution. *J. Incl. Phenom. Macrocycl. Chem.* 40, 213–219. doi: 10.1023/A:1011820513256
- Omorogie, M. O., Babalola, J. O., Unuabonah, E. I., Song, W., and Gong, J. R. (2016). Efficient chromium abstraction from aqueous solution using a low-cost biosorbent: nauclea diderrichii seed biomass waste. *J. Saudi Chem. Soc.* 20, 49–57. doi: 10.1016/j.jscs.2012.09.017
- Rao, K. V., Jain, A., and George, S. J. (2014). Organic-inorganic light-harvesting scaffolds for luminescent hybrids. *J. Mater. Chem. C* 2, 3055–3064. doi: 10.1039/C3TC31729C
- Scholtzová, E., Madejová, J., and Tunega, D. (2016). Structural and spectroscopic characterization of montmorillonite intercalated with n-butylammonium cations (n= 1–4)—Modeling and experimental study. *Clays Clay Miner.* 64, 401–412. doi: 10.1346/CCMN.2016.0640404
- Širić, I., Kasap, A., Bedeković, D., and Falandysz, J. (2017). Lead, cadmium and mercury contents and bioaccumulation potential of wild edible saprophytic and ectomycorrhizal mushrooms, Croatia. *J. Environ. Health Part B* 52, 156–165. doi: 10.1080/03601234.2017.1261538
- Soewu, D. A., Agbolade, O. M., Oladunjoye, R. Y., and Ayodele, I. A. (2014). Bioaccumulation of heavy metals in cane rat (*Thryonomys swinderianus*) in Ogun State, Nigeria. *J. Toxicol. Environ. Health Sci.* 6, 154–160. doi: 10.5897/JTEHS2014.0310
- Talbi, H., Humbert, B., and Billaud, D. (1998). FTIR and Raman spectroscopic investigations on the redox behaviour of poly (5-cyanoindole) in acidic aqueous solutions. *Spectrochim. Acta A Mol. Biomol. Spectr.* 54, 1879–1893. doi: 10.1016/S1386-1425(98)00146-2
- Tian, G., Wang, W., Wang, D., Wang, Q., and Wang, A. (2017). Novel environment friendly inorganic red pigments based on attapulgite. *Powder Technol.* 315, 60–67. doi: 10.1016/j.powtec.2017.03.044
- Tournassat, C., Bourg, I. C., Holmboe, M., Sposito, G., and Steefel, C. I. (2016). Molecular dynamics simulations of anion exclusion in clay interlayer nanopores. *Clays Clay Miner.* 64, 374–388. doi: 10.1346/CCMN.2016.0640403
- Wang, F. X., Liu, Y. D., and Pan, G. B. (2011). Vapor growth and photoconductivity of single-crystal nickel-phthalocyanine nanorods. *Mater. Lett.* 65, 933–936. doi: 10.1016/j.matlet.2010.12.012
- Wang, G., Wang, S., Sun, W., Sun, Z., and Zheng, S. (2017). Synthesis of a novel illite@ carbon nanocomposite adsorbent for removal of Cr (VI) from wastewater. *J. Environ. Sci.* 57, 62–71. doi: 10.1016/j.jes.2016.10.017
- Wang, J., Hu, Y., Deng, R., Xu, W., Liu, S., Liang, R., et al. (2012). Construction of multifunctional photonic crystal microcapsules with tunable shell structures by combining microfluidic and controlled photopolymerization. *Lab. Chip* 12, 2795–2798. doi: 10.1039/C2LC40419B
- Wang, M., He, L., Xu, W., Wang, X., and Yin, Y. (2015). Magnetic assembly and field-tuning of ellipsoidal-nanoparticle-based colloidal photonic crystals. *Angew. Chem. Int. Edn.* 54, 7077–7081. doi: 10.1002/anie.201501782
- Wang, W., Tian, G., Zong, L., Zhou, Y., Kang, Y., Wang, Q., et al. (2017). From illite/smectite clay to mesoporous silicate adsorbent for efficient removal of chlortetracycline from water. *J. Environ. Sci.* 51, 31–43. doi: 10.1016/j.jes.2016.09.008
- Wei, X., Hao, T., Xu, Y., Lu, K., Li, H., Yan, Y., et al. (2016). Facile polymerizable surfactant inspired synthesis of fluorescent molecularly imprinted composite sensor via aqueous CdTe quantum dots for highly selective detection of  $\lambda$ -cyhalothrin. *Sens. Actuat. B Chem.* 224, 315–324. doi: 10.1016/j.snb.2015.10.048
- Weibel, G., Waber, H. N., Eggenberger, U., and Mäder, U. K. (2016). Influence of sample matrix on the alkaline extraction of Cr (VI) in soils and industrial materials. *Environ. Earth Sci.* 75:548. doi: 10.1007/s12665-015-5236-3
- Wu, L., Liao, L., Lv, G., and Qin, F. (2015a). Stability and pH-independence of nano-zero-valent iron intercalated montmorillonite and its application on Cr (VI) removal. *J. Contam. Hydrol.* 179, 1–9. doi: 10.1016/j.jconhyd.2015.05.001
- Wu, L., Lv, G., Liu, M., Li, Z., Liao, L., and Pan, C. (2015b). Adjusting the layer charges of host phyllosilicates to prevent luminescence

- quenching of fluorescence dyes. *J. Phys. Chem. C* 119, 22625–22631. doi: 10.1021/acs.jpcc.5b07243
- Wu, L. M., Tong, D. S., Li, C. S., Ji, S. F., Lin, C. X., Yang, H. M., et al. (2016). Insight into formation of montmorillonite-hydrochar nanocomposite under hydrothermal conditions. *Appl. Clay Sci.* 119, 116–125. doi: 10.1016/j.clay.2015.06.015
- Xu, W., Mu, B., and Wang, A. (2016). From adsorbents to electrode materials: facile hydrothermal synthesis of montmorillonite/polyaniline/metal oxide (hydroxide) composites. *New J. Chem.* 40, 2687–2695. doi: 10.1039/C5NJ03734D
- Yan, D., Lu, J., Chen, L., Qin, S., Ma, J., Wei, M., et al. (2010a). A strategy to the ordered assembly of functional small cations with layered double hydroxides for luminescent ultra-thin films. *Chem. Commun.* 46, 5912–5914. doi: 10.1039/C0CC00522C
- Yan, D., Lu, J., Ma, J., Wei, M., Wang, X., Evans, D. G., et al. (2010b). Anionic poly (p-phenylenevinylene)/layered double hydroxide ordered ultrathin films with multiple quantum well structure: a combined experimental and theoretical study. *Langmuir* 26, 7007–7014. doi: 10.1021/la904228b
- Yu, W. H., Li, N., Tong, D. S., Zhou, C. H., Lin, C. X. C., and Xu, C. Y. (2013). Adsorption of proteins and nucleic acids on clay minerals and their interactions: a review. *Appl. Clay Sci.* 80–81, 443–452. doi: 10.1016/j.clay.2013.06.003
- Yu, W. H., Ren, Q. Q., Tong, D. S., Zhou, C. H., and Wang, H. (2014). Clean production of CTAB-montmorillonite: formation mechanism and swelling behavior in xylene. *Appl. Clay Sci.* 97–98, 222–234. doi: 10.1016/j.clay.2014.06.007
- Yusof, A. M., and Malek, N. A. (2009). Removal of Cr (VI) and As (V) from aqueous solutions by HDTMA-modified zeolite Y. *J. Hazard. Mater.* 162, 1019–1024. doi: 10.1016/j.jhazmat.2008.05.134
- Zamojć, K., Wiczak, W., Zaborowski, B., Jacewicz, D., and Chmurzynski, L. (2015). Fluorescence quenching of 7-amino-4-methylcoumarin by different TEMPO derivatives. *Spectrochim. Acta Part A Mol. Biomol. Spectrosc.* 136, 1875–1880. doi: 10.1016/j.saa.2014.10.102
- Zhang, H., Wang, C., Li, M., Ji, X., Zhang, J., and Yang, B. (2005). Fluorescent nanocrystal–polymer composites from aqueous nanocrystals: methods without ligand exchange. *Chem. Mater.* 17, 4783–4788. doi: 10.1021/cm050260l
- Zhou, C. H., Zhao, L. Z., Wang, A. Q., Chen, T. H., and He, H. P. (2016). Current fundamental and applied research into clay minerals in China. *Appl. Clay Sci.* 119, 3–7. doi: 10.1016/j.clay.2015.07.043

**Conflict of Interest Statement:** The authors declare that the research was conducted in the absence of any commercial or financial relationships that could be construed as a potential conflict of interest.

Copyright © 2018 Wei, Mei, Li, Liu, Lv, Weng, Liao, Li and Lu. This is an open-access article distributed under the terms of the Creative Commons Attribution License (CC BY). The use, distribution or reproduction in other forums is permitted, provided the original author(s) and the copyright owner(s) are credited and that the original publication in this journal is cited, in accordance with accepted academic practice. No use, distribution or reproduction is permitted which does not comply with these terms.